Regular Article

PHYSICAL CHEMISTRY RESEARCH
Published by the
Iranian Chemical Society
www.physchemres.org
info@physchemres.org

Phys. Chem. Res., Vol. 9, No. 1, 31-42, March 2021
DOI: 10.22036/pcr.2020.228364.1765

Complexation of Modified Deferasirox with Iron Cation in Three-multiplicities: A Theoretical Study on the [SPION-APTMS-DFX-Fe] Nanostructure

S.M. Mashmoul Moghadam, A. Shokooh Saljooghi and M. Izadyar*
Department of Chemistry, Faculty of Science, Ferdowsi University of Mashhad, Mashhad, Iran
(Received 24 April 2020, Accepted 22 September 2020)

Iron is one of the most important elements in biological systems and related processes to the oxygen transfer. Although the inadequate level of iron leads to physical disability, a high level of iron also plays a role in several diseases, including heart disease, diabetes and cancer. Iron chelators are species that facilitate iron removal. Experimental results have shown that iron chelators have strong antiplatelet properties against many cancers. In this study, for the first time, Deferasirox is conjugated to the superparamagnetic iron oxide nanoparticles (SPIONs) with the aid of APTMS linker, yielding iron-ligand complex (ligand = SPION-APTMS-DFX). The terminal methyl groups are considered as the substitutes for nanoparticles. Theoretical calculations were performed at M062X/6-311G(d,p) level to obtain the optimized structures of the iron complex in quintet, triplet, and singlet multiplicities. Natural bond orbital and quantum theory of atoms in molecules analyses were carried out to understand the nature of the complex bond character and electronic transitions in the complexes. The obtained results confirm a high affinity of Deferasirox to iron and show that the bond of metal ion and donor atoms of the ligand is covalent.

Keywords: Chelation therapy, DFX, SPION, Iron-ligand

INTTRODUCTION

One of the most important nanoparticles that are of great interest to researchers is the superparamagnetic iron oxide nanoparticles (SPIONs) [1]. SPINs are the only metal oxide nanoparticles approved for the clinical trials that have a great potential in various biomedical applications, such as magnetic resonance imaging (MRI) [2], targeted drug or gene delivery [3], tissue engineering [4], magnetic transfections [5], iron detection [6] and chelation therapy [7]. Modifying surface properties in SPIONs is a powerful tool for targeted drug delivery [3].

Iron is one of the most important elements that are particularly useful for many tasks in the human body, including the high variability reductive potential of Fe^{2+}/Fe^{3+}, which can be well regulated by the type of selected ligand. The ligand-iron complexes can have potentials in the biological range (from -0.5 mv to + 0.6 mv) [8]. If iron is not properly bonded to proteins in body, it may participate in harmful free radical reactions (Fenton or Haber-Weiss) or hydrolysis [9]. Living organisms adapt efficient storage and transport mechanisms for the safe handling of iron and prevention of toxicity of free unbound iron. Since the human body does not have an effective iron disposal system, the depletion of iron sources due to exfoliation is related to mucosal cells and red blood cells. The iron balance is mainly determined by the iron uptake, so the iron uptake increases due to the decrease in iron stores [10].

The term "iron overload" refers to the condition that excess iron is stored in human body. Excess iron is mainly found in the parenchymal tissue in the liver, heart, and endocrine system, causing injury and ultimately organ failure [11]. Chelation therapy has been used for many years to treat iron overload in the body using chelators that are selective and have a high tendency to absorb iron and

*Corresponding author. E-mail: izadyar@um.ac.ir

are excreted through the urine and feces [12].

Chelation therapy involves the use of ligand-capable drugs that are highly bonded to iron that are used to treat diseases caused by iron overload. By the coordination of these ligands to intracellular and extracellular iron, removal of this intermediate metal from biological systems is promoted [13]. Deferasirox is a tridentate chelator containing triazolyl nitrogen and two phenolic oxygen as donor groups. Deferasirox has been accepted by the FDA in fall 2005 and is meantime in use in more than 70 countries [14]. Considering the Deferasirox usage in medicine, the stability constants of the Deferasirox complexes with Al^{3+}, Mg^{2+}, Ca^{2+}, Fe^{2+}, Fe^{3+}, Cu^{2+} and Zn^{2+} have been recently determined [15]. To gain a more comprehensive understanding of sophisticated experimental measurements and to guide novel experimental investigations, it is necessary to study the relationship between the biological and nanoparticle domains in terms of theoretical calculations [16]. It should be noted that in previous studies, the thermodynamic equilibrium constants related to the iron-chelating by Deferasirox have been studied theoretically. Due to time and cost management, as well as the possible harms associated with excessive consumption of drugs on the body, to avoid spending time and cost, firstly, it should be confirmed through theoretical calculations and then focuses on project implementation in laboratory and clinic [17]. In this project, the peripheral carboxylate group closed by APTMS linker [FeL] can be protonated once. Thus L^{2-} acts as a bidentate coordinating ligand, somewhere binding of the metal center happens through the two phenolate groups and one of the nitrogen atoms of the heterocycle. However, there has been a big effort to recognize these chelator actions to reduce the Fe concentration in the clinical investigates; however, there are little attempts carried out to understand the mechanism of these compounds as a chelator, theoretically [18,19].

Although several works have been carried out on DFO-Fe and Deferiprone-Fe complexes [20], there are a few reports about the Deferasirox-Fe complex based on our knowledge [18,19,21]. The main reason for conducting this theoretical study is that the presence of toxic metals daily entering the body is one of the problems of industrial life. One of these toxic metals is iron, which is removed from the body by Deferasirox in this project. Since theoretical calculations are a prelude to laboratory and clinical tests, an attempt has been made to examine this project in theory so that in the case of obtaining the desired results, in the same research group, practical experiments are of interest. Considering the high capacity of nanoparticles and Deferasirox, this research aims at a comprehensive study on the high affinity and specificity of the nanoparticle-Deferasirox-Fe and predicting the equilibrium constant of their complexes in the gas phase and solvent (water). Finally, the chemical properties of the obtained complex, bonding properties, and electron transfer were investigated using the NBO (natural bond orbital) [22] and QTAIM (quantum theory of atoms in molecules) approaches [23]. As discussed, compounds containing SPIONs are known as one of the newest research fields in recent years. This is because compounds containing SPIONs are used as contrast agents in MRI to diagnose and treat diseases. In this study, to synthesize a compound containing a contrast agent and a therapeutic agent, for the first time, Deferasirox was placed on the SPION substrate using APTMS linker. The promising results obtained encouraged us to synthesize this compound *in vitro* and evaluate its diagnostic and therapeutic effects.

The presence of SPIONs in the studied complex leads to binding the drug to the desired tissue. Another reason for doing this project is to achieve a combination for use as targeted delivery, which is one of the newest areas of research, recently [24,25].

THEORETICAL METHODS

All quantum chemistry calculations were performed using the Gaussian 09 computational package. To simplify and decrease the computational cost, a 1:1 molar ratio of the Fe ion to DFX was considered in all complexes. DFT calculations were used to optimize the structures of the DFX and their complexes with Fe^{2+}. All calculations were performed using the M062X/6-311G(d) level of theory.

To estimate the zero-point vibrational energies as well as the corresponding thermodynamic parameters, frequency calculations were performed. Solvation Gibbs energies and solvent effects were calculated by the polarizable continuum model (PCM) [26]. The NBO analysis was applied to explore the distribution of the electrons into the molecular

orbitals and appropriate scheme for the analysis of the donor-acceptor interactions [27]. QTAIM analysis [28] was performed to elucidate the nature and strength of the bonding interactions of different complexes. To predict the effect of the solvent on the affinity of Deferasirox ligand to Fe^{2+} ion, solvent-solute interactions were calculated in the gas phase and water.

RESULTS AND DISCUSSION

Structural Analysis

Optimized structures of the studied L (SPION-APTMS-DFX) and Fe-L complexes are depicted in Fig. 1. It is important to be noted that the iron complexes were considered in three states of quintet, singlet, and triplet multiplicity for iron with the multiplicities of 5, 1 and 3, respectively. Table S1 shows the geometrical parameters of the L-Iron complexes. The main structural parameters of the complexes, reported in Table S1, are the Fe-O and Fe-N distances and O-Fe-O and O-Fe-N angles, indicating an efficient interaction between the Fe ion and oxygen/nitrogen atoms of Deferasirox. The obtained results show that in the [FeL] complex, the presence of solvent has not an important effect on the bond lengths in all complexes. The bonding angles of O2-Fe-N4 and O3-Fe-N4 (for atom numbering see Fig. 1) decrease in the solvent in the quintet multiplicity, whereas the bond angles in the singlet and triplet multiplicity modes did not change significantly that are in good agreement with the experimental results. The reason for this behavior is that in the quintet multiplicity, the electrons enter the eg orbitals that are in the Z-axis direction leading to increase in the bond length. Increasing the length of the bond will create a spatial barrier and the structure will reduce the bond angle to counter this spatial structure [18,19]. Also, the angles of O69-Fe-O71 and O2-Fe-O3 are about 180°, and O2-Fe-N4 and O67-Fe-O71 angles are close to 90° in the obtained complexes indicating that these complexes have an octahedral structure.

Equilibrium Constants

The formation of the Fe(II)-L complexes was investigated and the results of the equilibria studies are summarized in Table 1. Thermodynamic parameters of the complex formation reactions show their exothermic nature in the gas phase and water ($\Delta H^{298} < 0$). Negative characters of ΔH^{298} confirm that Fe-L binding is an enthalpy driven process [29]. ΔG^{298} values show the spontaneous nature of the complex formation.

According to Table 1, the reactivity of the Deferasirox in different multiplicities of Fe^{2+} is according to triplet > singlet > quintet, in the gas phase, and triplet > quintet > singlet in the solvent, confirming a greater affinity of Deferasirox towards Fe^{2+} in the triplet multiplicity. Higher stability constants of the [Fe-L] complexes in the triplet multiplicity show a greater affinity of the ligand towards Fe^{2+}. Furthermore, these values confirm that all complexes are more stable in the gas phase than water in the triplet multiplicity.

In the case of 1:1 complexes, the equilibrium equation can be shown by Eq. (1) and the stability constant values ($\log K_1$) are calculated according to Eq. (2).

$$Fe^{2+} + L^{2-} \leftrightarrow FeL \quad (1)$$

$$\log K_1 = \frac{-\Delta G}{2.303RT} \quad (2)$$

NBO Analysis

NBO analysis was used to quantify the metal cation atomic charges, the occupancy of atomic orbitals, and the atomic orbital contributions to the molecular orbitals. This analysis is also used in studies for determination of the electronic charges on the atoms at the center of the complexes and estimation of the main donor-acceptor interactions. Therefore, NBO analysis was performed on the optimized structures. In this analysis, the electronic wave function is elucidated in terms of the occupied Lewis and unoccupied Lewis localized orbitals. The strength of the donor-acceptor energies, E(2), is evaluated by the second-order perturbation theory [30], which is due to the delocalization of electrons from the donor to the acceptor. The main donor-acceptor interaction energies of the complexes are related to the interaction of the lone pair electrons of the oxygen atom of the chelator (LP_O) and antibonding orbital (LP*) of the Fe^{2+}, represented in Table 2. The stronger donor-acceptor interaction is equal to the higher interaction energy values, showing a greater charge transfer from the oxygen atom of the ligand (donor)

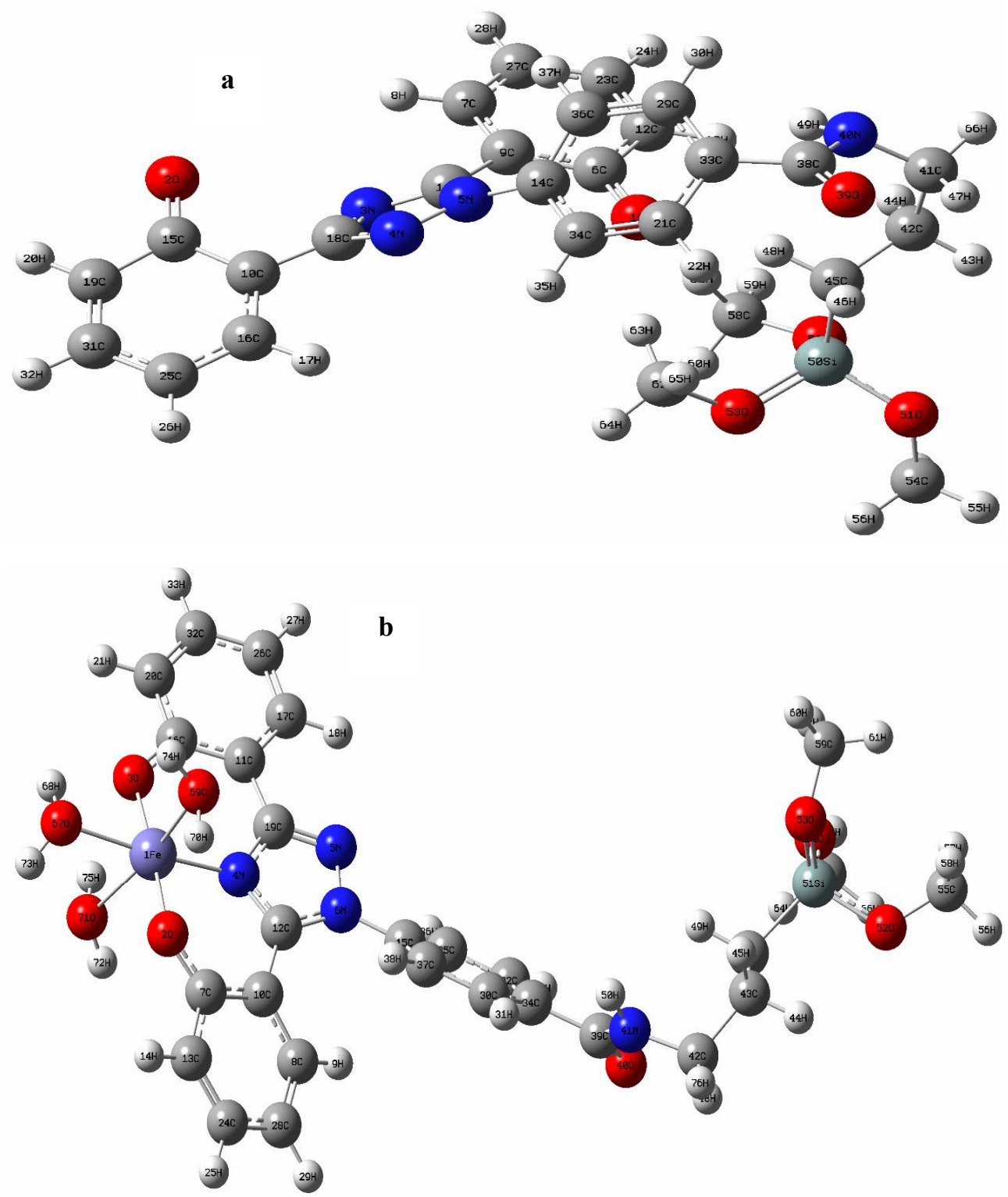

Fig. 1. Optimized structures of (a) Deferasirox (L^{2-}) and (b) [FeL].

Table 1. The Calculated logK Value for NP-APTMS-Fe(II)-Deferasirox Complexes

logK	Gas phase			Water		
	Quintet multiplicity	Triplet multiplicity	Singlet multiplicity	Quintet multiplicity	Triplet multiplicity	Singlet multiplicity
$logK_1$[FeL]	0.6040	0.6282	0.6244	0.4164	0.4312	0.0854
ΔH (kJ)	-1292.00	-1335.32	-1325.87	-862.73	-879.27	-147.55
ΔG (kJ)	-1371.82	-1426.69	-1418.03	-945.70	-979.31	-194.00
ΔS (J mol^{-1} k^{-1})	-64.44	-73.89	-74.13	-71.90	-79.89	-71.80

Table 2. Significant Donor-acceptor Interactions of the NP-APTMS-Fe(II)-Deferasirox Complex in Different Media within the Second-order Perturbation Stabilization Energies, E(2), (kcal mol^{-1})

Natural bond orbital interactions		E(2) (Quintet multiplicity)		E(2) (Singlet multiplicity)		E(2) (Triplet multiplicity)		
Donor	Acceptor	Gas-phase	Water	Gas-phase	Water	Gas-phase	Water	
LP_{O2}	LP^*_{Fe}	21.96	21.52	96.41	88.99	35.7	32.78	[FeL]
LP_{O3}	LP^*_{Fe}	7.83	14.68	101.43	92.96	37.58	35.36	
LP_{N4}	LP^*_{Fe}	12.85	11.56	80.13	75.31	36.2	34.79	
LP_{O67}	LP^*_{Fe}	11.19	11.31	60.22	61.97	24.86	27.3	
LP_{O69}	LP^*_{Fe}	11.42	12.21	69.83	70.13	8.77	8.78	
LP_{O71}	LP^*_{Fe}	9.85	10.22	70.07	73.01	7.88	9.6	
LP_{O2}	LP^*_{Fe}	14.35	14.86	54.59	60.39	13.82	12.59	$[Fe(H_2O)_6]^{2+}$
LP_{O4}	LP^*_{Fe}	14.29	14.89	55.27	51.32	19.23	21.99	
LP_{O6}	LP^*_{Fe}	14.31	14.91	37.89	58.51	13.61	27.08	
LP_{O8}	LP^*_{Fe}	13.78	14.87	54.61	60.75	13.83	12.59	
LP_{O10}	LP^*_{Fe}	14.03	14.87	55.32	61.52	19.24	21.99	
LP_{O12}	LP^*_{Fe}	13.88	14.88	37.88	58.59	13.61	27.09	

to the metal ion (acceptor). In the case of [FeL], the interaction between the lone pair electron of the oxygen (LP_{O3}) atom and antibonding orbital of the metal ion (LP^*_{Fe}) is strong at the singlet multiplicity than the triplet and quintet multiplicities. This value in singlet and triplet multiplicities and in the gas phase is greater than that in corresponding multiplicities in solvent while in quintet multiplicity, this value in solvent is greater than that in gas phase.

According to the obtained results, the metal center is considered as a strong electron acceptor and the metal ion-coordinated atoms (O and N) as the electron donors to iron ion. The rate of electron transfer from the nitrogen and oxygen atoms to the central atom is nearly equal in all multiplicities, confirming that the coordinated iron is a divalent ligand.

According to the NBO results, the main interactions in the [FeL] complexes are related to electron transfer from the non-bonding electrons of the oxygen atoms (LP_{O2}) to the anti-bonding orbitals of Fe^{2+} (LP^*_{Fe}) in the singlet multiplicity, non-bonding electrons of the oxygen atoms (LP_{O3}) to the anti-bonding orbitals of the iron atom (LP^*_{Fe}) in the singlet multiplicity, non-bonding electrons of the oxygen atoms (LP_{O3}) to the anti-bonding orbitals of the iron atom (LP^*_{Fe}) in the triplet multiplicity. The electronic charge transport is affected by the solvent, therefore the amount of interaction energies is different in the gas phase and water.

DFT Reactivity Indices

The highest occupied molecular orbital- lowest unoccupied molecular orbital (HOMO-LUMO) analysis was performed to evaluate the DFT reactivity indices. Based on this analysis, the electronic chemical hardness, η, electronic chemical potential, μ, and the global electrophilicity index, ω, were calculated [31]. Electronic chemical hardness (η) [32], defined as the resistance to electron cloud change of a chemical molecule, is defined according to Eq. (3):

$$\eta = \frac{1}{2}(E_{LUMO-E_{HUM}}) \quad (3)$$

The tendency to separate electrons from the ground state of a species is determined by the chemical electron potential (μ) [33], expressed by Eq. (4):

$$\mu = \frac{1}{2}(E_{HUMO+E_{LUMO}}) \quad (4)$$

The global electrophilicity index, ω [34], that indicates the relationship between η and μ, is also determined according to Eq. (5):

$$\omega = \frac{\mu^2}{2\eta} \quad (3)$$

The results are presented in Table 3. Also, the frontier molecular orbitals of the complex in all multiplicities in the gas phase and solvent were investigated and are illustrated in Figs. 2 and 3, respectively. The complex in the quintet multiplicity has the lowest energy gap and highest electronic chemical hardness. The lower energy gap for the complex in the quintet multiplicity indicates that the interactions between the ligand atoms and the metal ion are affected by the charge transfer interaction more than the electrostatic interactions. It is worth noting that the presence of solvent leads to an increase in the HOMO-LUMO gap in the quintet and triplet multiplicity, indicating that the solvent hurts the chelating process. The increase in η, due to the presence of solvent, leads to an instability of the complex. The electrophilicity of the free ligand is lower than that of the complex. The higher electrophilicity index for the quintet multiplicity shows that it was less inclined to form the complex with Fe^{2+}, whereas the singlet and triplet multiplicites have a similar tendency to form the complex.

QTAIM Analysis

QTAIM introduced by Bader characterizes the chemical bonding of a system based on the topological parameters at the bond critical point (BCP), such as electron density (ρ(r)) and Laplacian of the electron density (L(r)). This analysis was performed to study the effect of solvents on the strength of interactions [35]. QTAIM analysis at the BCPs was performed on the [Fe-L] and $[Fe(H_2O)_6]^{2+}$ complexes, at three multiplicities in the gas phase and water. The results of the topological analysis for the electronic charge density of the reactants and products at the BCPs including the values of the electron density (ρ(r)) for [FeL] and

Table 3. HOMO-LUMO Energies and Energy Gap of Complexes (a.u.) in Singlet, Triplet and Quintet Multiplicity in [Gas Phase] and {Solvent}

Complex	HOMO	LUMO	η	-μ	-ω
Singlet multiplicity	[-0.268]	[-0.218]	[0.025]	[0.243]	1.18
	{-0.268}	{-0.218}	{0.024}	{0.24}	1.18
Triplet multiplicity	[-0.231]	[-0.209]	[0.011]	[0.243]	2.68
	{-0.240}	{-0.211}	{0.014}	{0.225}	1.78
Quintet multiplicity	[-0.226]	[-0.211]	[0.007]	[0.218]	3.35
	{-0.230}	{-0.210}	{0.009}	{0.22}	2.66
Ligand	[-0.309]	[-0.208]	[0.050]	[0.258]	[0.659]
	{-0.311}	{-0.208}	{0.051}	{0.259}	{0.657}

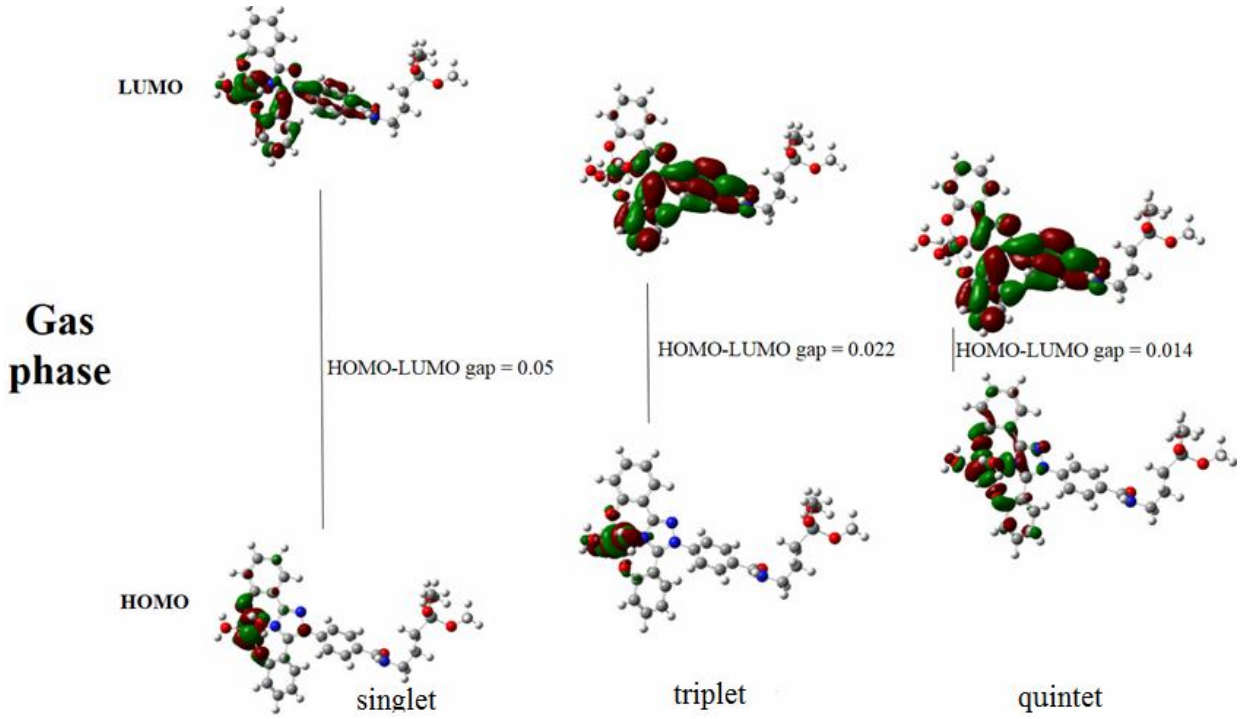

Fig. 2. Electron density distribution of boundary molecular orbitals of the complexes within the HOMO-LUMO gap (a.u.) in the gas phase.

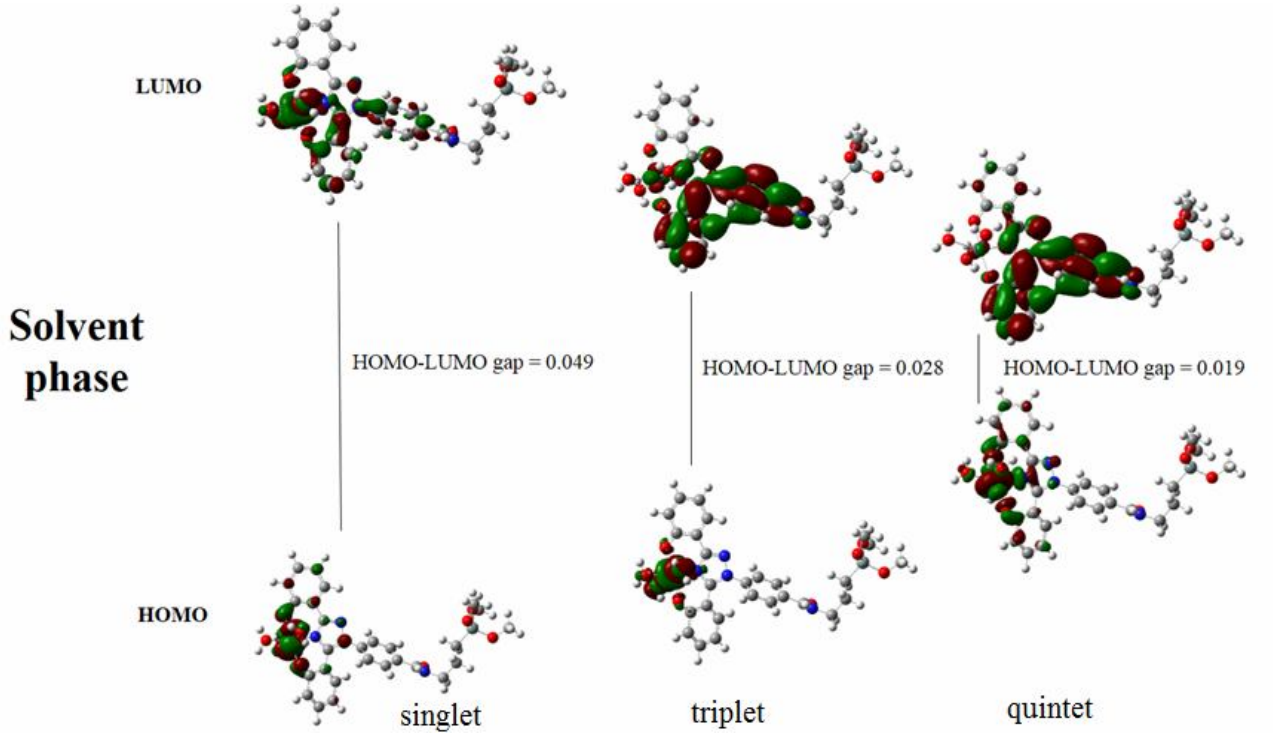

Fig. 3. Electron density distribution of boundary molecular orbitals of the complexes within the HOMO-LUMO gap (a.u.) in the solvent.

$[Fe(H_2O)_6]^{2+}$ complexes are summarized in Table 4. This table shows that the electron density values for the bonds involved in complexation are higher than the electron density values for these bonds in the free state, suggesting the interaction between the metal ion and the ligand. For example, ρ(r) values for Fe-O2 in the gas phase and water, in quintet multiplicity are 0.055 and 0.056 while after the complexation of ligand to Fe, these values increased to 0.076 and 0.075. Based on the ρ(r) value, the strength of the bond and the extent of bond formation between the ligand and Fe ion could be determined. The nature of the bond is also explained by Laplacian and H. The electronic charge density changes in the complex in different environments for the Fe-X bond (X = O, N) show the effect of the solvent. According to Table 4, in the case of [FeL], the electron density of Fe-N4 bond in triplet and singlet multiplicities in the gas phase and water, are greater than the other bonds, indicating that the strength of this interaction is the greatest at the complex which in turn confirms that the Fe-N bond is stronger than Fe-O. The ratio of the potential energy density to the kinetic energy density, |V|/G, is used as a parameter to describe the nature of the bond [36]. If this ratio is greater than one, it indicates the covalent nature of the bond. In all cases, the calculated value of ρ(r) is positive in the [FeL] complexes, which indicates the formation of an effective bond between the metal and drug [37]. The electron density decreases in the presence of the solvent for the Fe-N bond in comparison with the Fe-O bond confirming that the Fe-N bond is stronger than Fe-O. For example, the value of this quantity for Fe-N4 bond in the gas phase and quintet multiplicity is 0.063 and in the solvent is 0.059, while this quantity for Fe-O2 bond in the gas phase and the same multiplicity is equal to 0.076 and in the solvent is equal to 0.075. The comparison of these two bonds in the triplet multiplicity showed that the electron density changes from 0.086 to 0.083 by changing from the gas phase to the solvent for the Fe-N4 bond, while it does not change for the Fe-O3 bond (0.083), as shown in Table 4.

Table 4. Topological Properties (a.u.) for the Fe-X Bonds (X = O,N) in $[Fe(H_2O)_6]^{2+}$ and [FeL] Complexes in Different Spin States

			Gas			Water		
Quintet multiplicity	$[Fe(H_2O)_6]^{2+}$		ρ	L	|V|/G	ρ	L	|V|/G
		Fe-O2	0.055	-0.085	0.963	0.056	-0.089	0.976
		Fe-O4	0.054	-0.084	0.975	0.056	-0.088	0.976
		Fe-O6	0.054	-0.085	0.963	0.056	-0.089	0.976
		Fe-O8	0.052	-0.080	0.974	0.056	-0.089	0.976
		Fe-O10	0.053	-0.082	0.962	0.056	-0.088	0.976
		Fe-O12	0.053	-0.082	0.962	0.056	-0.088	0.976
	[FeL]							
		Fe-O2	0.076	-0.11	1.035	0.075	-0.110	1.026
		Fe-O3	0.069	-0.097	1.030	0.061	-0.084	1.011
		Fe-N4	0.063	-0.085	1.044	0.059	-0.080	1.036
		Fe-O67	0.045	-0.065	0.984	0.045	-0.064	0.983
		Fe-O69	0.050	-0.071	0.985	0.051	-0.081	0.974
		Fe-O71	0.044	-0.060	0.983	0.044	-0.064	0.984
Triplet multiplicity	$[Fe(H_2O)_6]^{2+}$		ρ	L	|V|/G	ρ	L	|V|/G
		Fe-O2	0.053	-0.091	0.966	0.049	-0.083	0.975
		Fe-O4	0.060	-0.111	0.962	0.064	-0.122	0.966
		Fe-O6	0.047	-0.090	0.963	0.053	-0.103	0.927
		Fe-O8	0.052	-0.091	0.955	0.049	-0.083	0.975
		Fe-O10	0.060	-0.111	0.962	0.064	-0.122	0.966
		Fe-O12	0.047	-0.090	0.927	0.053	-0.103	0.927
	[FeL]							
		Fe-O2	0.077	-0.129	1.022	0.073	-0.123	1.008
		Fe-O3	0.083	-0.139	1.034	0.083	-0.140	1.034
		Fe-N4	0.086	-0.150	1.068	0.083	-0.146	1.058
		Fe-O67	0.058	-0.108	0.971	0.058	-0.112	0.963
		Fe-O69	0.040	-0.054	0.981	0.040	-0.054	0.981
		Fe-O71	0.038	-0.048	1.000	0.040	-0.055	1.000
Singlet multiplicity	$[Fe(H_2O)_6]^{2+}$		ρ	L	|V|/G	ρ	L	|V|/G
		Fe-O2	0.041	-0.102	-0.09	0.060	-0.125	0.950
		Fe-O4	0.053	-0.132	-0.07	0.058	-0.124	0.949
		Fe-O6	0.043	-0.107	0.907	0.059	-0.124	0.957
		Fe-O8	0.041	-0.102	-0.09	0.060	-0.127	0.950
		Fe-O10	0.053	-0.132	-.073	0.060	-0.124	0.957
		Fe-O12	0.043	-0.106	-0.09	0.059	-0.124	0.957
	[FeL]							
		Fe-O2	0.069	-0.128	1.000	0.066	-0.127	0.984
		Fe-O3	0.074	-0.136	1.007	0.070	-0.143	0.985
		Fe-N4	0.084	-0.153	1.049	0.081	-0.146	1.045
		Fe-O67	0.056	-0.104	0.969	0.056	-0.111	0.952
		Fe-O69	0.057	-0.107	0.962	0.056	-0.108	0.961
		Fe-O71	0.055	-0.107	0.953	0.055	-0.110	0.946

Data Validity Analysis

To investigate the theoretical procedure applied in this project, the comparison of the obtained data with the reported results is of importance to have a reasonable understanding of the accuracy of the theoretical methods.

The calculated angles of O2-Fe-N4 and O3-Fe-N4 in the presence of solvent and in quintet multiplicity were reduced, which corresponds to the electron transmission into the eg orbitals. This behavior is in agreement with the reported data in previous work at high spin state [19].

In this work, the higher electrophilicity index for the quintet multiplicity shows a less tendency of complex formation with Fe^{2+}, whereas in the previous work [19], this quantity at high spin state is lower than low spin state.

Steinhauser and coworkers claimed that the rate of electron transfer from the nitrogen atoms due to the sp^2 hybrid must always be lower than that of oxygen, in the case of trivalent ion. If the oxygen atoms were coordinated to a trivalent ion, they would have higher electron transfer than nitrogen [38]. This observation contradicts our previous works with the same ligand [18,19], in which nitrogen atoms have sp^2 hybridization and their electron charge transfer is lower than that of oxygen atoms, indicating that they have a higher affinity for trivalent central metals, while in this project, the tendency to the divalent atom is preferred.

The QTAIM analysis shows that the amount of the ratios of the potential energy density to kinetic energy density for Fe-O2, Fe-O3, and Fe-N4 bonds in quintet and triplet multiplicities, in both of gas and solvent phases, are slightly more than one, indicating that the bonding between the central metal ion with O2, O3 and N4 atoms is covalent, which is in agreement with the previous project with the same ligand [18,19]. This shows that loading this drug on the SPION substrate will not affect the type of created bonds. In all multiplicities, the value of |V|/G decreases in the presence of the solvent, which is in agreement with the previous work with the same ligand, in the low spin state [19].

Based on the similarities and differences between different studies, it is well worth mentioning that the concept of the electron density and topological properties are good enough to predict the properties and behavior of the designed structures.

CONCLUSIONS

One of the most important chelators used to treat iron-overload related diseases is Deferasirox, a drug that selectively binds to the iron and removes it from the body. In this research, the thermodynamic aspects of ion chelating process was comprehensively studied using computational chemistry. Moreover, the effect of the substrate on the nature of bonding was investigated by simulating the substrate of superparamagnetic iron oxide nanoparticles and its binding to the drug. To this end, the effect of some variables, such as the solvent effects and spin states on the equilibrium constant of Deferasirox-iron complexes were analyzed. Based on the results, the solvent plays an important role in the reaction thermodynamics. The obtained results from the QTAIM analysis confirmed the covalent nature of the Deferasirox-iron bond and consequently high affinity of Deferasirox to iron. According to NBO studies, the electron transfer from the chelating atoms to Deferasirox was significantly affected by the solvent.

ACKNOWLEDGMENTS

The research council of Ferdowsi University of Mashhad is acknowledged for financial supports (Grant No. 3/43931).

REFERENCES

[1] Jain, T. K.; Morales, M. A.; Sahoo, S. K.; Leslie-Pelecky, D. L.; Labhasetwar, V., Iron oxide nanoparticles for sustained delivery of anticancer agents, *Mol. Pharm.,* **2005**, *2*, 194-205, DOI: 10.1021/mp0500014.

[2] Korchinski, D. J.; Taha, M.; Yang, R.; Nathoo, N.; Dunn, J. F., Iron Oxide as an MRI Contrast Agent for Cell Tracking, *Magn. Reson. Insights,* **2015**, *8*, 15-29, DOI: 10.4137/MRI.S23557.

[3] Peng, X. H.; Qian, X.; Mao, H.; Wang, A. Y.; Chen, Z. G.; Nie, S.; Shin, D. M., Targeted magnetic iron oxide nanoparticles for tumor imaging and therapy, *Int. J. Nanomedicine,* **2008**, *3*, 311-21, DOI: 10.2147/ijn.s2824.

[4] Mahmoudi, M.; Zhao, M.; Matsuura, Y.; Laurent, S.; Yang, P. C.; Bernstein, D.; Ruiz-Lozano, P.; Serpooshan, V., Infection-resistant MRI-visible scaffolds for tissue engineering applications, *BioImpacts*, **2016**, *6*, 111-115, DOI: 10.15171/bi.2016.16.

[5] Albukhaty, S.; Naderi-Manesh, H.; Tiraihi, T., *In vitro* labeling of neural stem cells with poly-L-lysine coated super paramagnetic nanoparticles for green fluorescent protein transfection, *Iranian Biomedical Journal*, **2013**, 17, 71-76, DOI: 10.6091/ibj.1114.2013.

[6] Singh, N.; Jenkins, G. J.; Asadi, R.; Doak, S. H., Potential toxicity of superparamagnetic iron oxide nanoparticles (SPION), *Nano Rev*, **2010**, *1*, 1-15, DOI: 10.3402/nano.v1i0.5358.

[7] Huang, G.; Chen, H.; Dong, Y.; Luo, X.; Yu, H.; Moore, Z.; Bey, E. A.; Boothman, D. A.; Gao, J., Superparamagnetic iron oxide nanoparticles: amplifying ROS stress to improve anticancer drug efficacy, *Theranostics*, **2013**, *3*, 116-26, DOI: 10.7150/thno.5411.

[8] Roelfes, G.; Vrajmasu, V.; Chen, K.; Ho, R. Y.; Rohde, J. U.; Zondervan, C.; La Crois, R. M.; Schudde, E. P.; Lutz, M.; Spek, A. L.; Hage, R.; Feringa, B. L.; Munck, E.; Que, L., End-on and side-on peroxo derivatives of non-heme iron complexes with pentadentate ligands: models for putative intermediates in biological iron/dioxygen chemistry, *Inorg. Chem.*, **2003**, *42*, 2639-53, DOI: 10.1021/ic034065p.

[9] Lyngsie, G.; Krumina, L.; Tunlid, A.; Persson, P., Generation of hydroxyl radicals from reactions between a dimethoxyhydroquinone and iron oxide nanoparticles, *Sci. Rep.*, **2018**, *8*, 10834-10843, DOI: 10.1038/s41598-018-29075-5.

[10] Burdo, J. R.; Connor, J. R., Brain iron uptake and homeostatic mechanisms: An overview, *Biometals*, **2003**, *16*, 63-75, DOI: 10.1023/a:1020718718550.

[11] Beerenhout, C.; Bekers, O.; Kooman, J. P.; van der Sande, F. M.; Leunissen, K. M. L., A comparison between the soluble transferrin receptor, transferrin saturation and serum ferritin as markers of iron state in hemodialysis patients, *Nephron*, **2002**, *92*, 32-35, DOI: 10.1159/000064468.

[12] Kang, H.; Han, M.; Xue, J.; Baek, Y.; Chang, J.; Hu, S.; Nam, H.; Jo, M. J.; El Fakhri, G.; Hutchens, M. P.; Choi, H. S.; Kim, J., Renal clearable nanochelators for iron overload therapy, *Nat. Commun.*, **2019**, *10*, 5134-5145, DOI: 10.1038/s41467-019-13143-z.

[13] Lamas, G. A., A new look at an old treatment for heart disease, particularly in diabetics, *Circulation*, **2015**, *131*, 505-506, DOI: 10.1161/circulationaha.114.010774.

[14] Moukalled, N. M.; Bou-Fakhredin, R.; Taher, A. T., Deferasirox: Over a decade of experience in thalassemia, *Mediterr J. Hematol. Infect. Dis*., **2018**, *10*, 2018066-2018079, DOI: e2018066 10.4084/MJHID.2018.066.

[15] Lebitasy, M.; Ampe, E.; Hecq, J. D.; Karmani, L.; Nick, H.; Galanti, L., Ability of deferasirox to bind iron during measurement of iron, *Clin. Chem. Lab. Med*., **2010**, *48*, 427-429, DOI: 10.1515/CCLM.2010.080.

[16] Hammarson, M.; Nilsson, J. R.; Li, S.; Beke-Somfai, T.; Andreasson, J., Characterization of the thermal and photoinduced reactions of photochromic spiropyrans in aqueous solution, J. *Phys. Chem. B*, **2013**, *117*, 13561-13571, DOI: 10.1021/jp408781p.

[17] Lovell, M. A.; Ehmann, W. D.; Markesbery, W. R., Laser microprobe analysis of brain aluminum in Alzheimer' disease, *Ann. Neurol*., **1993**, *33*, 36-42, DOI: 10.1002/ana.410330107.

[18] Salehi, S.; Izadyar, M.; Sh. Saljooghi, A., Interactions of deferasirox as a chelating agent with Al and Ga cations: A theoretical study on the $[M(DFX)_2]_3$-nanostructures, *Phys. Chem. Res.*, **2018**, *6*, 67-82, DOI: 10.22036/pcr.2017.94247.1404.

[19] Salehi, S.; Sh. Saljooghi, A.; Izadyar, M., A theoretical study on the electronic structures and equilibrium constants evaluation of deferasirox iron complexes, *Comput. Biol. Chem.*, **2016**, *64*, 99-106, DOI: 10.1016/j.compbiolchem.2016.05.010.

[20] Crisponi, G.; Nurchi, V. M.; Crespo-Alonso, M.; Sanna, G.; Zoroddu, M. A.; Alberti, G.; Biesuz, R., A speciation study on the perturbing effects of iron chelators on the homeostasis of essential metal ions, *PLoS one*, **2015**, *10*, 0133050-0133064, DOI:

10.1371/journal.pone.0133050.

[21] Dehghan, Gh.; Shaghaghi, M.; Sattari, S.; Jouyban, A., Interaction of human serum albumin with Fe(III)-deferasirox studied by multispectroscopic methods, *J. Lumin.*, **2014**, *149*, 251-257, DOI: 10.1016/j.jlumin.2014.01.047.

[22] Glendening, E. D.; Landis, C. R.; Weinhold, F., Natural bond orbital methods, *WIRES Comput. Mol. Sci.*, **2011**, *2*, 1-42, DOI: 10.1002/wcms.51.

[23] Kumar, P. S. V.; Raghavendra, V.; Subramanian, V., Bader's theory of atoms in molecules (AIM), *J. Chem. Sci.*, **2016**, *128*, 1527-1536, DOI: 10.1007/s12039-016-1172-3.

[24] Salehi, S.; Sh. Saljooghi, A.; Shiri, A., Synthesis, characterization and in vitro anticancer evaluations of two novel derivatives of deferasirox iron chelator, *Eur. J. Pharmacol.*, **2016**, *781*, 209-217, DOI: 10.1016/j.ejphar.2016.04.026.

[25] Farokhzad, O.; Cheng, j.; Tply, B.; Sherifi, I.; Jon, S.; Kantoff, Ph.; Richie, J.; Longer, R., Targeted nanoparticle-aptamer bioconjugates for cancer chemotherapy *in vivo*, *PANS*, **2006**, *103*, 6315-6320, DOI: 10.1073/pnas.0601755103.

[26] Mennucci, B., Polarizable continuum model, Wiley Interdiscip. *Rev. Comput. Mol. Sci.*, **2012**, *2*, 386-404, DOI: 10.1002/wcms.1086.

[27] Reed, A. E.; Curtiss, L. A.; Weinhold, F., Intermolecular interactions from a natural bond orbital, donor-acceptor viewpoint, *Chem. Rev.*, **1988**, *88*, 899-926, DOI: 10.1021/cr00088a005.

[28] Matta, C. F., Special issue: Philosophical aspects and implications of the quantum theory of atoms in molecules (QTAIM), *Found. Chem.*, **2013**, *15*, 245-251, DOI: 10.1007/s10698-013-9194-0.

[29] Caro, J. A.; Harpole, K. W.; Kasinath, V.; Lim, J.; Granja, J.; Valentine, K. G.; Sharp, K. A.; Wand, A. J., Entropy in molecular recognition by proteins, *Proc. Natl. Acad. Sci.,* **2017**, *114*, 6563-6568, DOI: 10.1073/pnas.1621154114.

[30] Altas, E.; Tekin, B., Second order perturbation theory in general relativity: Taub charges as integral constraints, *Phys. Rev. D*, **2019**, *99*, 104078-104088, DOI: 10.1103/PhysRevD.99.104078.

[31] Garza, J.; Vargas, R.; Aquino, N.; Sen, K. D., DFT reactivity indices in confined many-electron atoms, *J. Chem. Sci.,* **2005**, *117*, 379-386, DOI: 10.1007/bf02708341.

[32] Mulliken, R. S., A new electroaffinity scale; together with data on valence states and on valence ionization potentials and electron affinities, *J. Chem. Phys.*, **1934**, *2*, 782-793, DOI: 10.1063/1.1749394.

[33] Parr, R. G.; Donnelly, R. A.; Levy, M.; Palke, W. E., Electronegativity: The density functional viewpoint, *J. Chem. Phys*., **1978**, *68*, 3801-3807, DOI: 10.1063/1.436185.

[34] Domingo, L. R.; Aurell, M. J.; Pérez, P.; Contreras, R., Quantitative characterization of the local electrophilicity of organic molecules. Understanding the regioselectivity on diels-alder reactions, *J. Phys. Chem. A*, **2002**, *106*, 6871-6875, DOI: 10.1021/jp020715j.

[35] Feng, Y., Cancer Chemotherapy: Time for new solution, *Chemotherapy*, **2014**, *03*, DOI: 10.4172/2167-7700.1000130.

[36] Nick, H.; Acklin, P.; Lattmann, R.; Buehlmayer, P.; Hauffe, S.; Schupp, J.; Alberti, D., Development of tridentate iron chelators: From desferrithiocin to ICL670, *Curr. Med. Chem*. **2003**, *10*, 1065-1076, DOI: 10.2174/0929867033457610.

[37] Rodrigues-Serrano, A.; Daza, M.; Doerr, M.; Villaveces, J., proton transfer from 1,4-penthadiene to superoxide radical anion: a QTAIM analysis, *Revista Colomb. Quim.,* **2012**, *41*, 409- 432, DOI: 10.15446/rev.colomb.quim.

[38] Steinhauser, S.; Heinz, U.; Bartholomä, M.; Weyhermüller, T.; Nick, H.; Hegetschweiler, K., Complex formation of ICL670 and related ligands with FeIII and FeII, *Eur. J. Inorg. Chem*, **2004**, *2004*, 4177-4192, DOI: 10.1002/ejic.200400363.